



NRL Report 9370

Convergence Performance of Adaptive Detectors Part 3

KARL GERLACH

*Target Characteristics Branch
Radar Division*

March 25, 1992

REPORT DOCUMENTATION PAGE			Form Approved OMB No. 0704-0188	
<small>Public reporting burden for this collection of information is estimated to average 1 hour per response, including the time for reviewing instructions, searching existing data sources, gathering and maintaining the data needed, and completing and reviewing the collection of information. Send comments regarding this burden estimate or any other aspect of this collection of information, including suggestions for reducing this burden, to Washington Headquarters Services, Directorate for Information Operations and Reports, 1215 Jefferson Davis Highway, Suite 1204, Arlington, VA 22202-4302, and to the Office of Management and Budget, Paperwork Reduction Project (0704-0188), Washington, DC 20503.</small>				
1. AGENCY USE ONLY (Leave blank)	2. REPORT DATE March 25, 1992	3. REPORT TYPE AND DATES COVERED Interim		
4. TITLE AND SUBTITLE Convergence Performance of Adaptive Detectors, Part 3		5. FUNDING NUMBERS PE - 61153N PR - 021-05-43 WU - DN480-006		
6. AUTHOR(S) Karl Gerlach				
7. PERFORMING ORGANIZATION NAME(S) AND ADDRESS(ES) Naval Research Laboratory Washington, DC 20375-5000		8. PERFORMING ORGANIZATION REPORT NUMBER NRL Report 9370		
9. SPONSORING / MONITORING AGENCY NAME(S) AND ADDRESS(ES) Office of Chief of Naval Research Arlington, VA 22217-5000		10. SPONSORING / MONITORING AGENCY REPORT NUMBER		
11. SUPPLEMENTARY NOTES				
12a. DISTRIBUTION / AVAILABILITY STATEMENT Approved for public release; distribution unlimited.		12b. DISTRIBUTION CODE		
13. ABSTRACT (Maximum 200 words) Two schemes for adaptive detection, Kelly's generalized likelihood ratio test (GLRT) and the mean level adaptive detector (MLAD), are analyzed with respect to the deleterious effect of desired signal contamination of the data used to compute the sampled covariance matrix for the two detectors. The detection probability P_D and false alarm performance (ghosting probability P_G) are predicted for the two schemes under the assumptions that the input noises are Gaussian random variables that are temporally independent but spatially correlated; and the desired signal's amplitude is Rayleigh distributed. P_D and P_G are computed as a function of the false alarm probability P_F with no contamination, the number of input channels, the number of independent samples-per-channel, the matched filtered output signal-to-noise (S/N) power ratio, and the S/N power ratio of the contaminating desired signal. It is shown that both P_D and P_G decrease with increasing levels of contamination. The P_G performance is almost identical for the GLRT and MLAD. The P_D performance shows similar relative performance trends. Significantly, it is shown that the ghosting probability does not exceed P_F in the presence of contamination.				
14. SUBJECT TERMS ECCM Adaptive filter Adaptive cancellation Adaptive detector			15. NUMBER OF PAGES	
			16. PRICE CODE 27	
17. SECURITY CLASSIFICATION OF REPORT UNCLASSIFIED	18. SECURITY CLASSIFICATION OF THIS PAGE UNCLASSIFIED	19. SECURITY CLASSIFICATION OF ABSTRACT UNCLASSIFIED	20. LIMITATION OF ABSTRACT SAR	

CONTENTS

1.0	INTRODUCTION	1
2.0	GENERALIZED LIKELIHOOD RATIO TEST	2
2.1	Detector Form	2
2.2	Statistically Equivalent GLRT	4
2.3	Probability of Detection	5
2.4	Probability of Ghosting	7
3.0	MEAN LEVEL ADAPTIVE DETECTOR	8
3.1	Detector Form and Statistically Equivalent MLAD	8
3.2	Probability of Detection	10
3.3	Probability of Ghosting	11
4.0	RESULTS	11
5.0	SUMMARY	21
6.0	REFERENCES	22
	APPENDIX — The Probability Density Function (PDF) of η	23

CONVERGENCE PERFORMANCE OF ADAPTIVE DETECTORS

PART 3

1.0 INTRODUCTION

In Ref. 1, two schemes for adaptive detection were compared: Kelly's generalized likelihood ratio test (GLRT) [2] and the mean level adaptive detector (MLAD). Detection performance P_D was predicted for the two schemes under the assumptions that the input noises are zero-mean Gaussian random variables that are temporally independent but spatially correlated, and the desired signal's amplitude is Rayleigh distributed. P_D was computed as a function of the false alarm probability, the number of input channels, the number of independent samples-per-channel, and the matched filtered output signal-to-noise (S/N) power ratio. The GLRT was shown to have better detection performance than the MLAD. The difference in detection performance increased as one used fewer input samples; however, the required number of samples necessary to have only a 3 dB detection loss for both detection schemes is approximately the same. This is significant since, for the present, the MLAD is considerably less complex to implement than the GLRT.

The general problem of signal detection in a background of Gaussian noise for an adaptive array was first addressed by Kelly [2] by using the techniques of statistical hypothesis testing. In Ref. 2, the problem is formulated as a binary hypothesis test where one hypothesis is noise only and the other is signal-plus-noise. A given input data vector (called the primary data vector) is tested for signal presence. Another set of signal-free data vectors (called the secondary data vectors) is available that shares the unknown covariance matrix \mathbf{M} of the noise in the primary data vector. A likelihood ratio decision rule was derived, and its performance was evaluated for the two hypothesis.

Kelly's detector uses the maximum likelihood (ML) estimates for the unknown parameters of the likelihood ratio test (LRT). The unknown parameters are the spatial covariance matrix and the unknown signal's complex amplitude (assumed in Kelly's analysis to be a nonrandom constant). This detection scheme is commonly referred to as the GLRT and is referenced in this report as such.

A less complex adaptive detection scheme is found by implementing MLAD. The MLAD is essentially an adaptive matched filter (AMF) followed by a mean level detector (MLD) [3,4]. Input samples used in determining the MLD threshold are derived from a block of data passing through the AMF. This same block of data is used to calculate the AMF weights. The squared magnitude of each of these same samples as processed through the AMF is used as a test statistic and compared against an MLD threshold (an average of the instantaneous powers) that does not contain the given test statistic sample. We further clarify the implementation terminology by calling this an MLAD with concurrent data samples. In Ref. 5, an analysis was performed for an MLAD with nonconcurrent data, i.e., the block of data that passes through the AMF that is used to determine the MLD threshold is statistically independent of the block of data used to calculate the AMF weights.

We note for both Kelly's GLRT and the MLAD that, under the above stated assumptions, the P_F does not depend on \mathbf{M} (a second order characterization of the external noise environment). Hence

detectors exhibit the desirable constant false alarm rate (CFAR) property of having the P_F be independent of the covariance matrix.

Here we extend the results of Ref. 1 to include the effects of what we term "desired signal contamination." By this, we mean that a significant level of a desired signal is present in the secondary data vectors, which, for both Kelly's GLRT and the MLAD, are used to estimate the unknown covariance matrix \mathbf{M} . We assume that the contaminating desired signal is statistically independent of the desired signal in the primary data vector. In practice, contamination can be caused by a variety of mechanisms, such as for the radar problem, multiple target returns being present at different ranges of the pulse compressor output. In this case, a number of the multiple target returns at distinct times that have the desired signal's waveform may be in the secondary data.

For our analysis, we simplify the contamination model by only considering a single source of contamination. In addition, this single source contaminates only one sample vector of the secondary data vectors. Two performance measures are affected: P_D and P_F . Because P_F is normally chosen under the condition of no contamination, we redesignate the probability of false alarm in the presense of contamination as the ghosting probability P_G . We do this since ghosts (in the radar sense) are desired signal-induced false detections.

Here we present results on the detection and ghosting performance of GLRT and MLAD in the presence of contamination. As in Ref. 1, we assume that the complex desired signal amplitude is a complex zero-mean Gaussian random variable (r.v.) of unknown variance with independent and identically distributed (i.i.d.) real and imaginary parts (the magnitude of this amplitude is Rayleigh distributed). Under the GLRT, we would have to reformulate Kelly's detector with the variance of the unknown signal amplitude as an unknown parameter, and find the ML estimate of this quantity. This proved to be mathematically tedious. In lieu of implementing this new GLRT, we choose to evaluate Kelly's GLRT, as it is defined in his paper. As noted by Kelly, no optimality properties are claimed for this test. The form of the test is, however, reasonable.

2.0. GENERALIZED LIKELIHOOD RATIO TEST

2.1 Detector Form

A mathematical formulation of the adaptive detection problem that leads to the GLRT is given by Kelly [2]. We now summarize that formulation. Two sets of input data are used, called the primary and secondary inputs. The secondary inputs are assumed not to contain the desired signal. Set

- X = $N \times K$ matrix of secondary input data. The n th row represents the K samples of data on the n th channel, where $n = 1, 2, \dots, N$. The samples in the k th column are assumed time-coincident.
- \mathbf{x} = primary data vector of length N .
- \mathbf{s} = desired steering vector of length N .

Consider the two hypothesis:

$$H_0 : \mathbf{x} = \mathbf{n}, \text{ and} \quad (1)$$

$$H_1 : \mathbf{x} = \mathbf{n} + a \mathbf{s}, \quad (2)$$

where H_0 is the noise only hypothesis, \mathbf{n} is a noise vector of length N , H_1 is the signal-plus-noise hypothesis, and a is the unknown complex signal amplitude. We make the following assumptions:

- (A1) Input noises are complex zero-mean stationary Gaussian r.v.'s. The real and imaginary parts of a given input noise sample are i.i.d. with respect to each other (an r.v. with these characteristics is called a circular Gaussian process).
- (A2) Input noise samples are temporally statistically independent.
- (A3) The secondary data is statistically independent of the primary data.
- (A4) $K \geq N$.

The GLRT is formulated as follows. The joint probability density function (PDF) under each hypothesis over all measured data is found. For this problem, this is straightforward, since the sample vectors are assumed independent and each vector has an associated N -dimensional Gaussian PDF. If there are any unknown parameters, the PDF of the inputs is maximized over all unknown parameters separately for each of the two hypotheses. The maximizing parameter values are by definition the ML estimators of the parameters. Hence the maximized PDFs are obtained by replacing the unknown parameters by their ML estimates. The ratio of the resultant maximum of PDFs is found (the ratio of the PDF under H_1 to the PDF under H_0). This ratio is checked to see if it exceeds a preassigned threshold t .

Kelly shows that the GLRT for the adaptive detection problem is given by

$$\frac{|s^H \hat{R}_x^{-1} \mathbf{x}|^2}{(s^H \hat{R}_x^{-1} s)[1 + \mathbf{x}^H \hat{R}_x^{-1} \mathbf{x}]} \underset{H_0}{\overset{H_1}{>}} t, \quad (3)$$

where

$$\hat{R}_x = \mathbf{X}\mathbf{X}^H, \quad (4)$$

and H denotes the conjugate transpose matrix operation. We recognize \hat{R}_x as proportional to the ML estimate of the input covariance matrix. We note also that the desired signal's unknown complex amplitude a has been estimated and is accounted for in Eq. (3). The elements of \hat{R}_x are r.v.'s that are functions of the input samples (the elements of \mathbf{X}). It is straight-forward to show that the probabilistic measure of the set of \mathbf{X} , for which \hat{R}_x is singular, is zero. Hence, when assessing detection performance, we can always assume that \hat{R}_x (or any other matrix that has the form given by Eq. (4)) is invertible.

For the signal contamination model, we make the additional assumption:

- (A5) A statistically independent desired signal is always present in the secondary data under H_0 or H_1 . It is only present on the K th sample vector (the K th column of \mathbf{X}).

For (A5), the choice of which secondary sample vector in time is contaminated is arbitrary and does not affect the analysis.

2.2 Statistically Equivalent GLRT

In Ref. 1, a statistically equivalent GLRT was derived that was used to formulate in simple fashion the P_D and P_F probabilities of the adaptive detector with no signal contamination. With one modification of the development in Ref. 1, we can derive a statistically equivalent GLRT that will allow us to formulate the P_D and P_G for the adaptive detector with signal contamination (which is modeled as given by (A5)). We briefly outline the methodology used to obtain the statistically equivalent GLRT.

As in Kelly's (and Reed, Mallet, and Brennan [6]) development, we can matrix transform the input vectors by an $N \times N$ matrix A , which has the properties that the input noise vectors are spatially whitened, each input element has noise power normalized to one, and

$$As = (0, 0, \dots, 0, (s^H M^{-1} s)^{1/2}) \equiv s_0, \quad (5)$$

where all of the desired signal has been placed into N th channel (note that in Kelly's paper, the signal was placed into the first channel; for our analysis, we place the signal into the N th channel).

In addition, set

$$z = Ax, \text{ and} \quad (6(a))$$

$$Z = AX. \quad (6(b))$$

The element of vector z (under H_0) and the elements of the vectors representing the columns of Z (each column represents the transformed secondary data across the array at a given instant of time) are now spatially independent with each element having power equal to 1. As shown by Kelly, the transformed GLRT is given by

$$\frac{|s_0^H \hat{R}_z^{-1} z|^2}{(s_0^H \hat{R}_z^{-1} s_0) (1 + z^H \hat{R}_z^{-1} z)} \underset{H_0}{\overset{H_1}{>}} t, \quad (7)$$

where

$$\hat{R}_z = ZZ^H. \quad (8)$$

We note that the desired signal contamination of the secondary data is completely contained in the N, K element of Z .

In Ref. 1, we show that by using a series of unitary matrix transformations ($K \times K$ transforms on Z and an $N \times N$ transform on z), the following statistically equivalent GLRT results:

$$\frac{|u_{11} v_2 - v_1 u_{21}|^2}{(u_{11}^2 + v_1^2) (u_{22}^2 + v_2^2)} \underset{H_0}{\overset{H_1}{>}} T, \quad (9)$$

where

$$T = \frac{t}{1-t}, \quad (10)$$

and $u_{11}, u_{21}, u_{22}, v_1$, and v_2 are independent r.v.'s. Furthermore, u_{11} has the χ PDF of order $2(K-N)$ with $\sigma^2 = 0.5$, v_1 has the χ PDF of order $2(N-1)$ with $\sigma^2 = 0.5$ under H_1 , v_2 is the sum of the desired signal in the primary data plus a circular Gaussian r.v. with power equal 1, and u_{21} is a circular Gaussian r.v. with power equal 1. In addition, if we adopt the notation of Ref. 1, then

$$u_{22}^2 = \sum_{k=N}^K |z_{Nk}^{(N-1)}|^2, \quad (11)$$

where $z_{Nk}^{(N-1)}$, $k = N, N+1, \dots, K-1$ are i.i.d. circular Gaussian r.v. with power equal 1 and $z_{Nk}^{(N-1)}$ is the sum of the contaminating desired signal plus a circular Gaussian r.v. with power equal 1.

We use the statistically equivalent GLRT given by Eq. (9) and the aforementioned probabilistic characterizations of $u_{11}, u_{21}, u_{22}, v_1$ and v_2 as the starting point for our analysis.

2.3 Probability of Detection

Under the H_1 hypothesis, we assume that the primary vector's desired signal's amplitude (or magnitude) is Rayleigh distributed and the signal's phase is uniformly distributed between $(0, 2\pi)$. This implies that the desired signal itself is a complex circular Gaussian r.v. Let the desired signal's input power-per-channel before any matrix transformation be equal to $\tilde{\sigma}_s^2$. After the A matrix transformation (whitening, normalizing, and placing the signal into the N th channel), the signal power in the N th channel is $\sigma_s^2 = \tilde{\sigma}_s^2 \mathbf{s}^H \mathbf{M}^{-1} \mathbf{s}$. Thus under H_1 , v_2 is a complex circular Gaussian r.v. with power equal to $\sigma_s^2 + 1$, where the 1 represents the noise power-level-per-channel after the A matrix transformation. In similar fashion, let the contaminating desired signal's input power-per-channel before any matrix transformation be equal to $\tilde{\sigma}_c^2$. Again we assume the contaminating desired signal's amplitude is Rayleigh distributed with phase uniformly distributed between $(0, 2\pi)$. After the A transformation, $\sigma_c^2 = \tilde{\sigma}_c^2 \mathbf{s}^H \mathbf{M}^{-1} \mathbf{s}$. Thus under H_0 or H_1 , $z_{Nk}^{(N-1)}$ is a complex circular Gaussian r.v. with power equal to $\sigma_c^2 + 1$, where again the 1 represents the noise power-level-per-channel after the A matrix transformation.

Recall that u_{21} is a complex circular Gaussian r.v. with power equal to 1. We can rewrite Eq. (9) as

$$\begin{array}{c} H_1 \\ |\alpha|^2 > T' \\ H_0 \end{array} \quad (12)$$

where

$$\alpha = \frac{u_{11}v_2 - v_1u_{21}}{(u_{11}^2(\sigma_s^2 + 1) + v_1^2)^{1/2}}, \text{ and} \quad (13)$$

$$T' = \frac{u_{11}^2 + v_1^2}{u_{11}^2(\sigma_s^2 + 1) + v_1^2} u_{22}^2 T. \quad (14)$$

It is straightforward to show that α , when conditioned on u_{11} and v_1 , is a complex circular Gaussian r.v. with power equal to 1. It is well known [7] that the conditional probability of detection is given by

$$P(D | u_{11}, u_{22}, v_1) = e^{-T'} = \exp \left\{ - \frac{u_{11}^2 + v_1^2}{u_{11}^2(\sigma_s^2 + 1) + v_1^2} u_{22}^2 T \right\}, \quad (15)$$

where $P(D | \cdot, \cdot)$ denotes the conditional probability of detection.

We set

$$\eta = u_{22}^2, \quad (16)$$

$$\mu = u_{11}^2, \quad (17)$$

$$v = v_1^2, \text{ and} \quad (18)$$

$$r = \frac{v}{\mu}. \quad (19)$$

Then Eq. (15) becomes

$$P(D | r, \eta) = \exp \left\{ - \frac{1 + r}{\sigma_s^2 + 1 + r} \eta T \right\}. \quad (20)$$

The PDFs of μ and N are χ^2 of order $2(K - N + 2)$ and $2(N - 1)$, respectively, with $\sigma^2 = 0.5$ and are given by

$$p_\mu(\mu) = \frac{1}{(K - N + 1)!} \mu^{K - N + 1} e^{-\mu}, \quad \mu \geq 0, \text{ and} \quad (21)$$

$$p_v(v) = \frac{1}{(N - 2)!} v^{N - 2} e^{-v}, \quad v \geq 0. \quad (22)$$

The PDF of η is derived in the Appendix and is given by

$$P_\eta(\eta) = \frac{1}{(\sigma_c^2 + 1)(K - N - 1)!} \eta^{K - N} e^{-\eta/(1 + \sigma_c^2)} \int_0^1 \lambda^{K - N - 1} \exp \left\{ - \lambda \eta \frac{\sigma_c^2}{\sigma_c^2 + 1} \right\} d\lambda, \quad \eta \geq 0. \quad (23)$$

By using elementary probability theory, it is straightforward to show that

$$p_r(r) = \int_0^\infty \frac{\beta}{r^2} p_v(\beta) p_\mu \left(\frac{\beta}{r} \right) d\beta. \quad (24)$$

By inserting expressions for p_μ and p_ν as given by Eq. (21) and (22), respectively, and simplifying results in the following expression for p_r :

$$p_r(r) = \frac{K!}{(N-2)!(K-N+1)!} \frac{r^{N-2}}{(1+r)^{K+1}}, r \geq 0. \quad (25)$$

If we set $q = 1/(1+r)$, it is straightforward to show that

$$p_q(q) = \frac{K!}{(N-2)!(K-N+1)!} (1-q)^{N-2} q^{K-N+1}, 0 \leq q \leq 1, \quad (26)$$

which is the PDF derived by Reed et al. [6] for the normalized instantaneous S/N power ratio and which results if the sampled matrix inversion (SMI) algorithm is used. By substituting q for r in Eq. (20),

$$p(D|q, \eta) = \exp - \left[\frac{1}{q \sigma_s^2 + 1} \right] \eta T. \quad (27)$$

If we multiply Eq. (27) by the PDF of η as given by Eq. (23) and integrate over the support of η , it is straightforward to show

$$p(D|q) = \frac{K-N}{\sigma_c^2 + 1} \int_0^1 \frac{\lambda^{K-N-1} d\lambda}{\left[\frac{T}{q \sigma_s^2 + 1} + \frac{1 + \lambda \sigma_c^2}{\sigma_c^2 + 1} \right]^{K-N+1}}. \quad (28)$$

Thus

$$P(D) = \int_0^1 p(D|q) p_q(q) dq, \quad (29)$$

where $p_q(q)$ is given by Eq. (26). We set $(S/N)_{opt} = \sigma_s^2$, where $(S/N)_{opt}$ is the optimal S/N output power ratio of the matched filter ($K = \infty$). We can write this in this way because the output noise power of the N th channel has been normalized to 1 and the output of the N th channel is the optimal matched filter output. We also set $(S/N)_{con} = \sigma_c^2$ where $(S/N)_{con}$ is the contaminated S/N output power ratio of the matched filter ($K = \infty$).

2.4 Probability of Ghosting

The probability of a ghost is easily derived from Eqs. (28) and (29) by setting $\sigma_s^2 = 0$. It is found that

$$P_G = \frac{K-N}{\sigma_c^2 + 1} \int_0^1 \frac{\lambda^{K-N-1} d\lambda}{\left[T + \frac{1 + \lambda \sigma_c^2}{1 + \sigma_c^2} \right]^{K-N+1}}. \quad (30)$$

If we set $\sigma_c^2 = 0$, then

$$P_G = P_F = \frac{1}{(T+1)^{K-N+1}}, \quad (31)$$

which is the probability of false alarm for the GLRT derived in Ref. 1 under the condition that there is no contamination.

3.0 MEAN LEVEL ADAPTIVE DETECTOR

3.1 Detector Form and Statistically Equivalent MLAD

In Ref. 1, an MLAD was formulated for the adaptive detection problem. In this subsection, we briefly review this formulation for the MLAD and give a statistically equivalent form that will be used to obtain results for P_D and P_G .

An intuitive form of adaptive detection is found by implementing the MLAD. The MLAD is essentially an AMF followed by an MLAD, as illustrated in Fig. 1. The MLAD is designed to perform detections over a block of data by using just this block of data in determining the AMF weights and the MLD threshold. The MLAD works as follows. Let there be N channel and $K + 1$ samples per channel. Define

\mathbf{x} = primary N -length data vector;

\mathbf{x}_k = secondary N -length data vector, $k = 1, 2, \dots, K$,

$X_{\text{aug}} = (\mathbf{x} | X)$ = augmented $N \times (K + 1)$ matrix of input data, and

$$\hat{R}_0 = X_{\text{aug}} X_{\text{aug}}^H.$$

The N -length weighting vector $\hat{\mathbf{w}}$ for the AMF is found by using the SMI algorithm and is given by

$$\hat{\mathbf{w}} = \hat{R}_0^{-1} \mathbf{s}. \quad (32)$$

This weight is used in the detection rule given by

$$\begin{array}{c} H_1 \\ |\hat{\mathbf{w}}^H \mathbf{x}|^2 > T_0 \sum_{k=1}^K |\hat{\mathbf{w}}^H \mathbf{x}_k|^2, \\ H_0 \end{array} \quad (33)$$

where T_0 is chosen to control the false alarm probability. We see that Eq. (32) is the algorithmic representation of the AMF and Eq. (33), the MLD.

Note that we have included the primary data vector in the \hat{R}_0 estimate and, hence, in the $\hat{\mathbf{w}}$ estimate. In a practical situation, this might be done, since it is more numerically efficient to compute one weighting vector over the entire data block than it is to compute a distinct weighting vector for each point in the block. However, the presence of the desired signal (under H_1) will affect detection. In Eq. (33), the primary data vector is varied across the $K + 1$ data snapshots, where the \mathbf{x}_k used on the right side of Eq. (33) does not include a selected primary data vector.

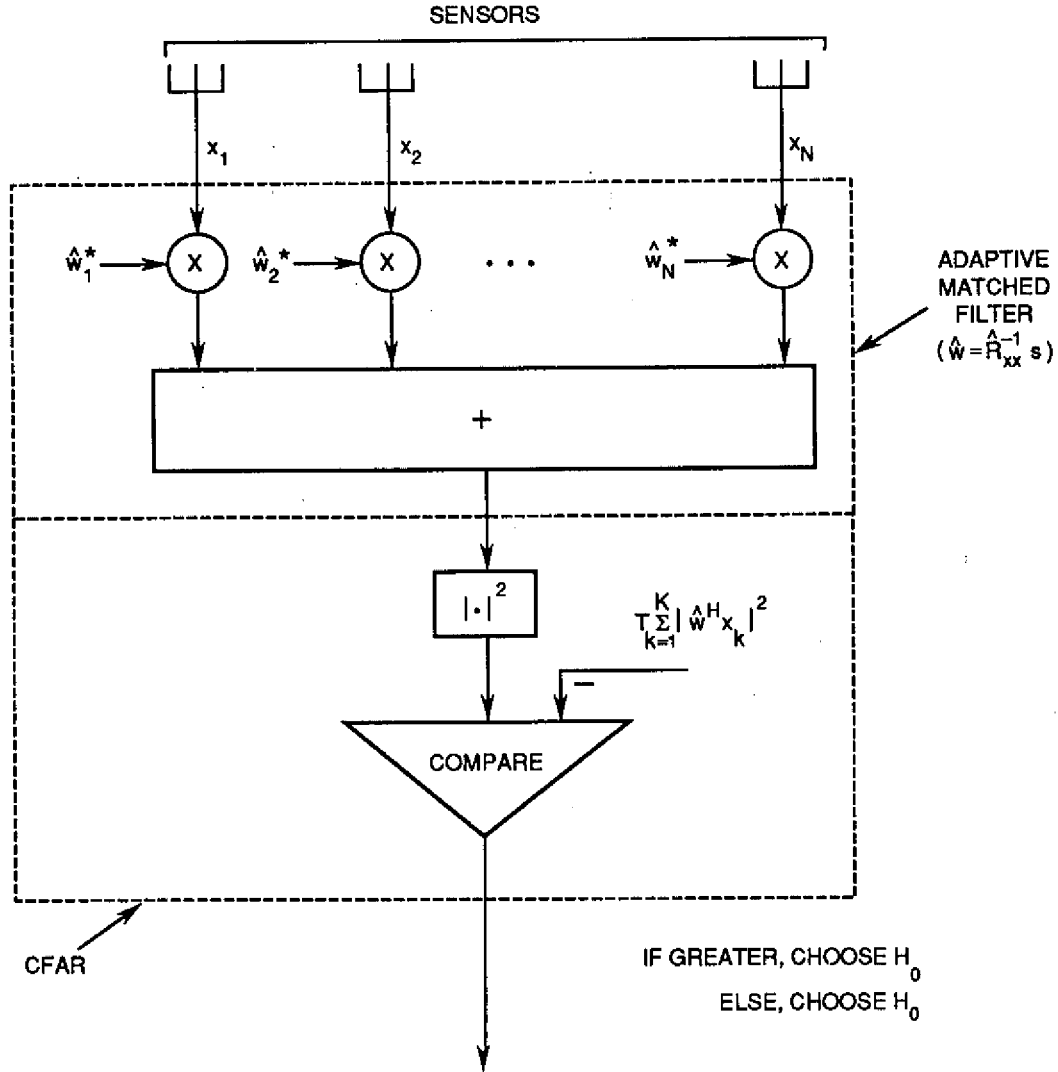


Fig. 1 — Mean level adaptive detector

In Ref. 1, it is shown that equivalent form of Eq. (33) is

$$\begin{matrix} H_1 \\ |s^H \hat{R}_x^{-1} x|^2 \\ H_0 \end{matrix} \begin{matrix} > \\ < \end{matrix} T_1 [(s^H \hat{R}_x^{-1} s)(1 + x^H \hat{R}_x^{-1} x)^2 + |s^H \hat{R}_x^{-1} x|^2 (1 + x^H \hat{R}_x^{-1} x)] , \quad (34)$$

where

$$T_1 = \frac{T_0}{T_0 + 1} , \quad (35)$$

and

$$\hat{R}_x = \hat{R}_0 - xx^H . \quad (36)$$

Also, $0 \leq T_1 \leq 1$.

Furthermore, it is shown in Ref. 1 that a statistically equivalent MLAD is given by

$$\left| u_{11}v_2 - v_1u_{21} \right|^2 \begin{matrix} H_1 \\ \left[1 - T_1 \left(1 + \frac{v_1^2}{u_{11}^2} \right) \right] \\ H_0 \end{matrix} \begin{matrix} > \\ < \end{matrix} \left(1 + \frac{v_1^2}{u_{11}^2} \right)^2 u_{11}^2 u_{22}^2 T_1, \quad (37)$$

where $u_{11}, u_{21}, u_{22}, v_1$, and v_2 are as probabilistically characterized in Section 2.2.

We note for $T_1 > 0$ that if

$$1 - T_1 \left(1 + \frac{v_1^2}{u_{11}^2} \right) \leq 0, \quad (38)$$

then H_0 is declared.

3.2 Probability of Detection

Again under the H_1 hypothesis, we assume the primary vector's desired signal and the contaminating desired signal are complex circular Gaussian r.v. (the amplitude is Rayleigh distributed). As in our analysis of the GLRT, $\sigma_s^2 = \tilde{\sigma}_s^2 \mathbf{s}^H \mathbf{M}^{-1} \mathbf{s}$ and $\sigma_c^2 = \tilde{\sigma}_c^2 \mathbf{s}^H \mathbf{M}^{-1} \mathbf{s}$. Assume Eq. (38) is not true. We can write the decision rule given by Eq. (37) as

$$\left| \alpha \right|^2 \begin{matrix} H_1 \\ > \\ < \\ H_0 \end{matrix} T'_1, \quad (39)$$

where

$$\alpha = \frac{u_{11}v_2 - v_1u_{21}}{(u_{11}^2(\sigma_s^2 + 1) + v_1^2)^{1/2}}, \quad (40)$$

$$T'_1 = \frac{1}{(q - T_1)(q \sigma_s^2 + 1)} \eta T_1, \quad (41)$$

η is defined by Eq. (16), and $q = (1 + r)^{-1}$. As before, under H_1 , v_1 is a complex circular Gaussian r.v. with power equal to $\sigma_s^2 + 1$, and u_{21} is the same with power equal to 1. Furthermore, α is the same with power equal to 1. Thus

$$P(D | q, \eta) = \begin{cases} 0 & \text{if } q \leq T_1 \\ e^{-T} & \text{otherwise.} \end{cases} \quad (42)$$

The PDFs of η and q are given by Eqs. (23) and (26), respectively. If we multiply $P(D | q, \eta)$ by $p_\eta(\eta)$ and integrate over the support of η , after some simplification, it will be found that for $q > T_1$,

$$P(D | q) = \frac{K-N}{\sigma_c^2 + 1} \int_0^1 \frac{\lambda^{K-N-1} d\lambda}{\left[\frac{T_1}{(q - T_1)(q\sigma_s^2 + 1)} + \frac{1 + \lambda\sigma_c^2}{1 + \sigma_c^2} \right]^{K-N+1}}. \quad (43)$$

Because $P(D | q) = 0$ for $q \leq T_1$, it follows that

$$P_D = \int_{T_1}^1 P(D | q) p_q(q) dq, \quad (44)$$

where $p_q(q)$ is given by Eq. (26). Again we set $(S/N)_{opt} = \sigma_s^2$ and $(S/N)_{con} = \sigma_c^2$.

3.3 Probability of Ghosting

The P_F is found by setting $(S/N)_{opt} = 0$ in Eq. (43). The following equations result:

$$P(G | q) = \begin{cases} \frac{K-N}{\sigma_c^2 + 1} \int_0^1 \frac{\lambda^{K-N-1} d\lambda}{\left[\frac{T_1}{q - T_1} + \frac{1 + \lambda\sigma_c^2}{1 + \sigma_c^2} \right]^{K-N+1}} & , q > T_1 \\ 0 & , q \leq T_1 \end{cases} \quad (45)$$

and

$$P_G = \int_{T_1}^1 P(G | q) p_q(q) dq. \quad (46)$$

If we set $\sigma_c^2 = 0$, it is straightforward to show that

$$P_G = P_F = (1 - T_1)^K, \quad (47)$$

which is the false alarm probability of the MLAD derived in Ref. 1 under the condition that there is no contamination.

4.0 RESULTS

Here we present results for the detection probability in contamination P_D and ghosting probability P_G for the GLRT and MLAD vs the independent parameters: the quiescent probability of false alarm (when there is *no* contamination) P_F ; the steady state ($K = \infty$) S/N output power ratio of the matched filter $(S/N)_{opt}$; the contaminated S/N power ratio $(S/N)_{con}$; the number of independent samples per channel K of secondary data; and the number of input channels N . We set $K = MN$, where M is a positive integer ≥ 2 , and use M instead of K as an independent parameter called the degrees-of-freedom factor.

Because there are many independent parameters, we present results for a representative set as shown in Figs. 2 through 19. Here we plot P_D and P_G vs $(S/N)_{con}$ for $N = 2, 5, 10, 30$; $P_F = 10^{-6}, 10^{-10}$, and $M = 2, 3, \dots, 6$. For plotting P_D , we choose $(S/N)_{opt}$ to equal either 20 dB or 30 dB, where a given $(S/N)_{opt}$ will yield a steady state ($K = \infty$) P_D , which is indicated by the horizontal line in Figs. 10 through 19. For plotting P_G in the steady state, $P_G = P_F$, which is indicated by horizontal line in Figs. 2 through 9.

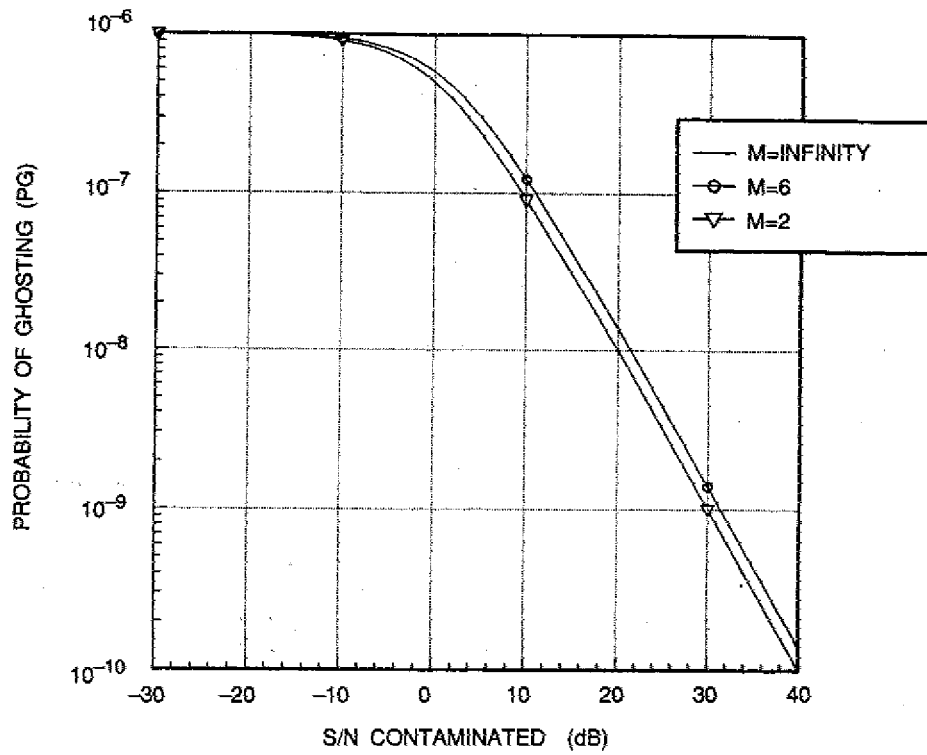


Fig. 2 — Kelly detector: PG for contaminated signal $N = 2$, $PF = 1.D-6$

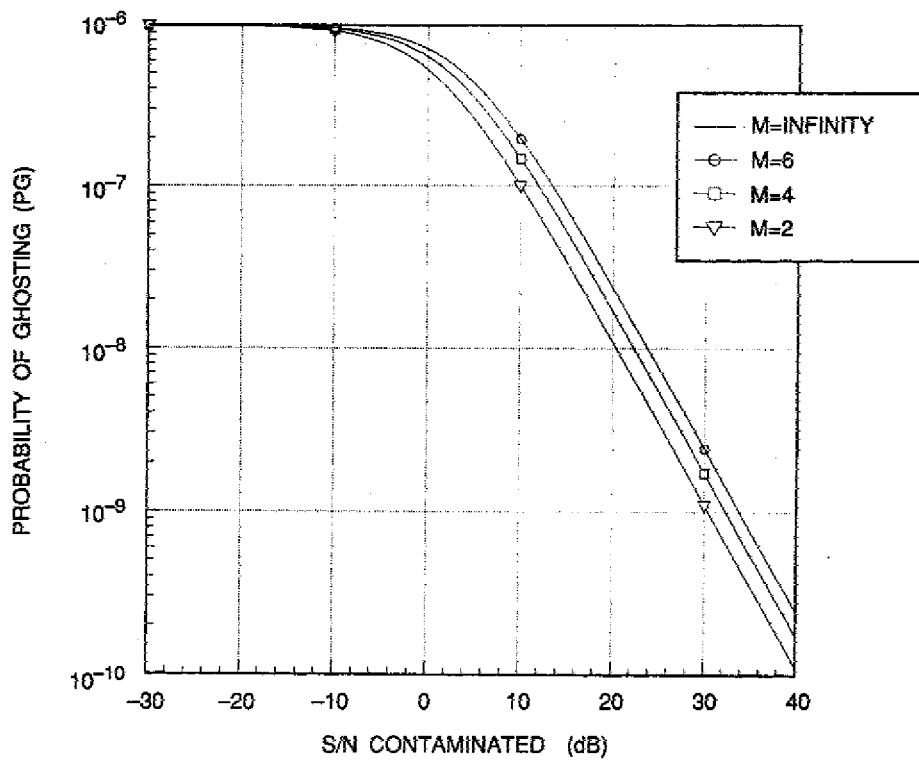


Fig. 3 — Kelly detector: PG for contaminated signal $N = 5$, $PF = 1.D-6$

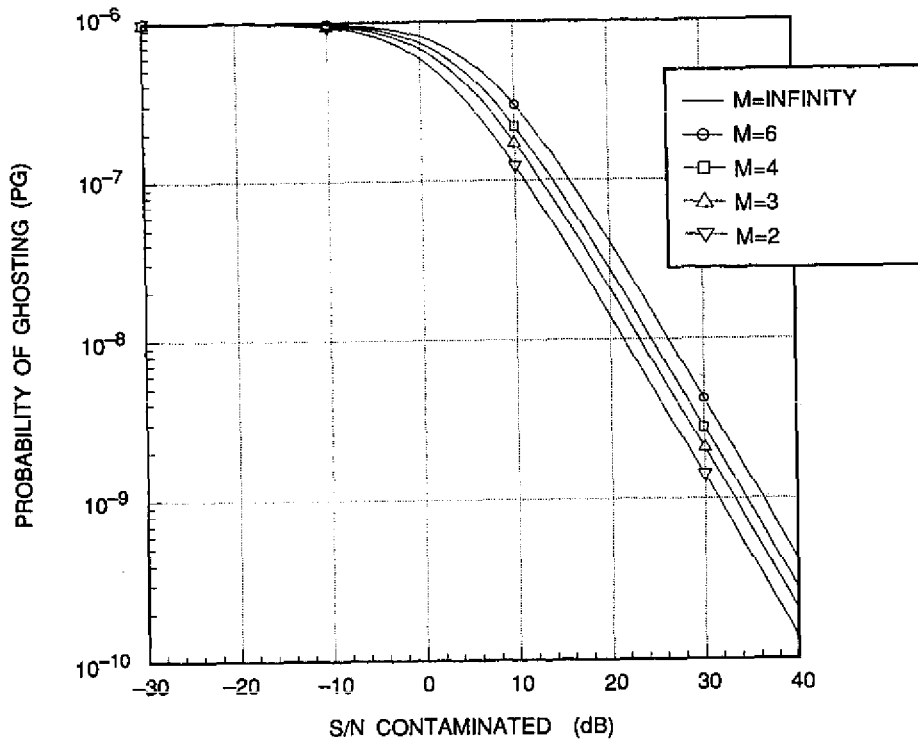


Fig. 4 — Kelly detector: PG for contaminated signal $N = 10$, $PF = 1.D-6$

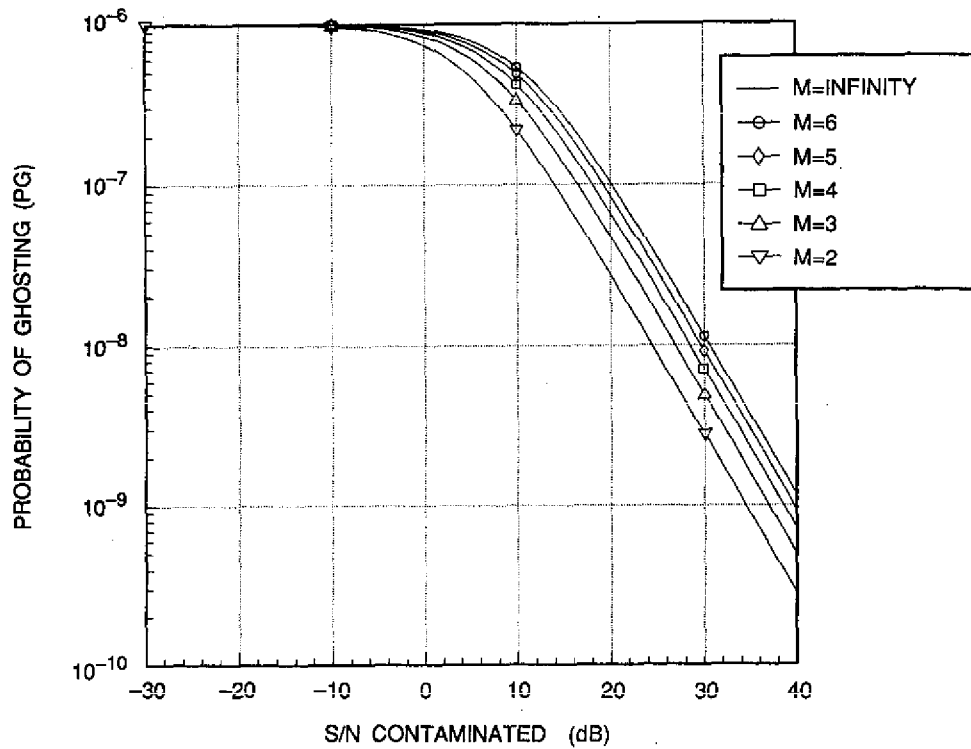


Fig. 5 — Kelly detector: PG for contaminated signal $N = 30$, $PF = 1.D-6$

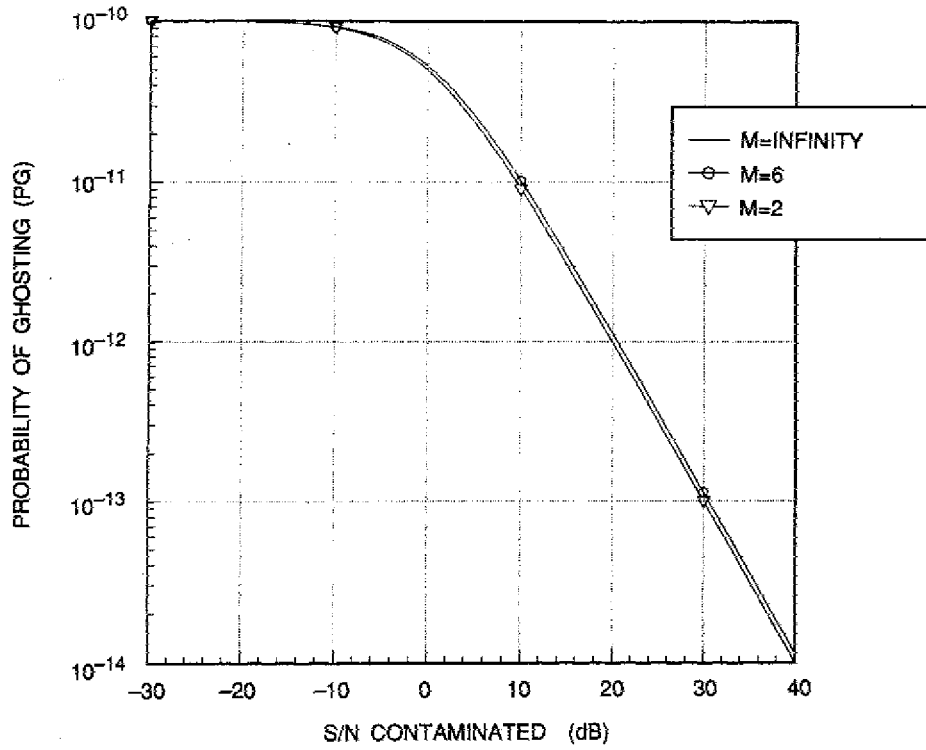


Fig. 6 — Kelly detector: PG for contaminated signal $N = 2$, $PF = 1.D-10$

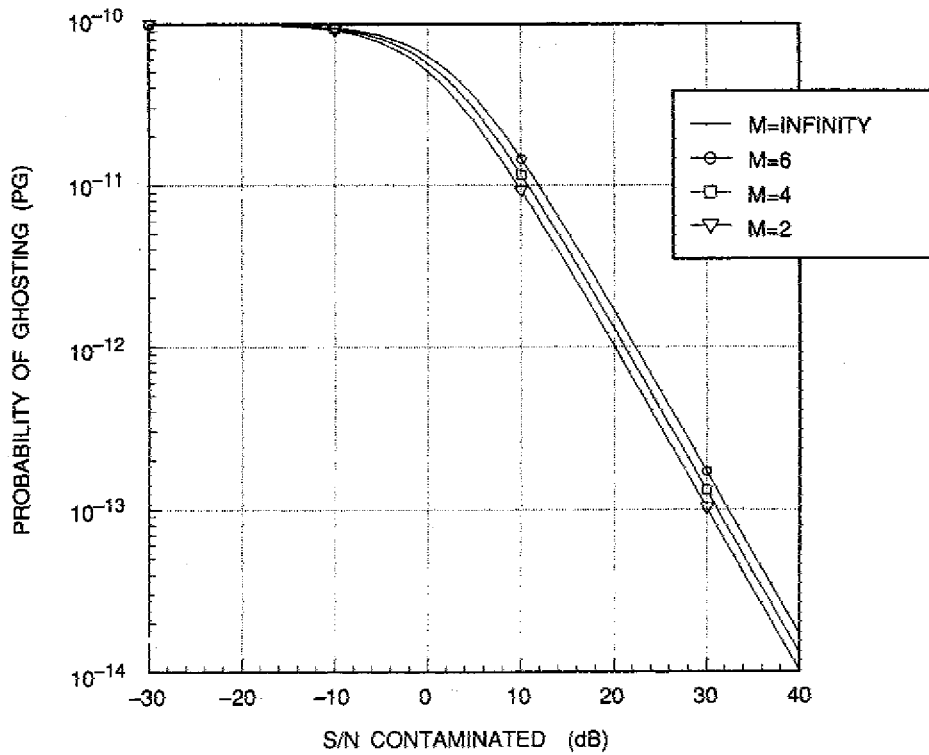


Fig. 7 — Kelly detector: PG for contaminated signal $N = 5$, $PF = 1.D-10$

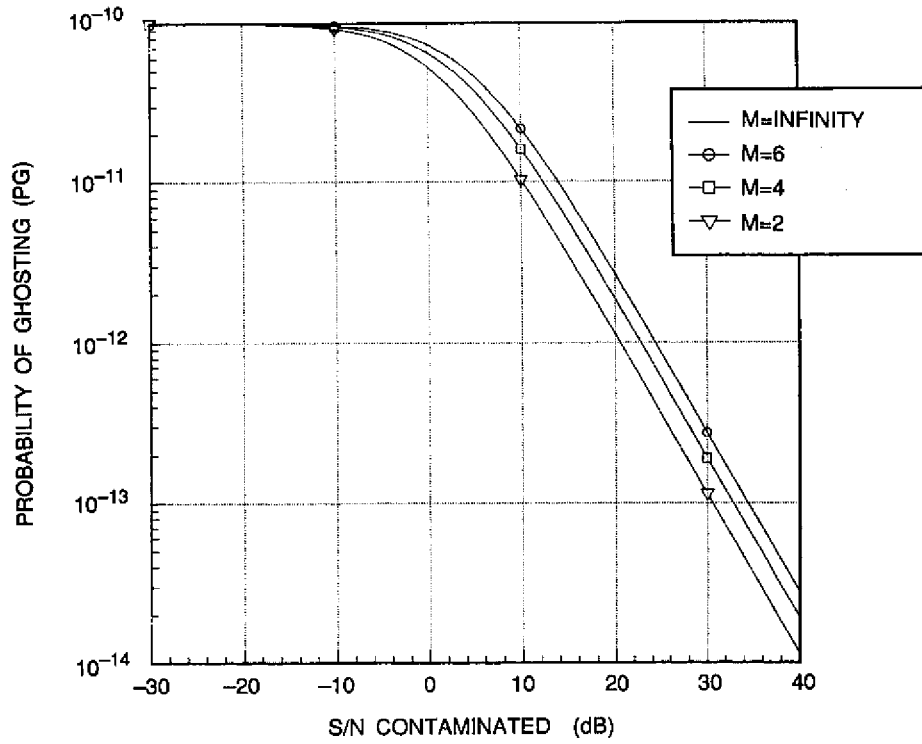


Fig. 8 — Kelly detector: PG for contaminated signal $N = 10$, $PF = 1.D-10$

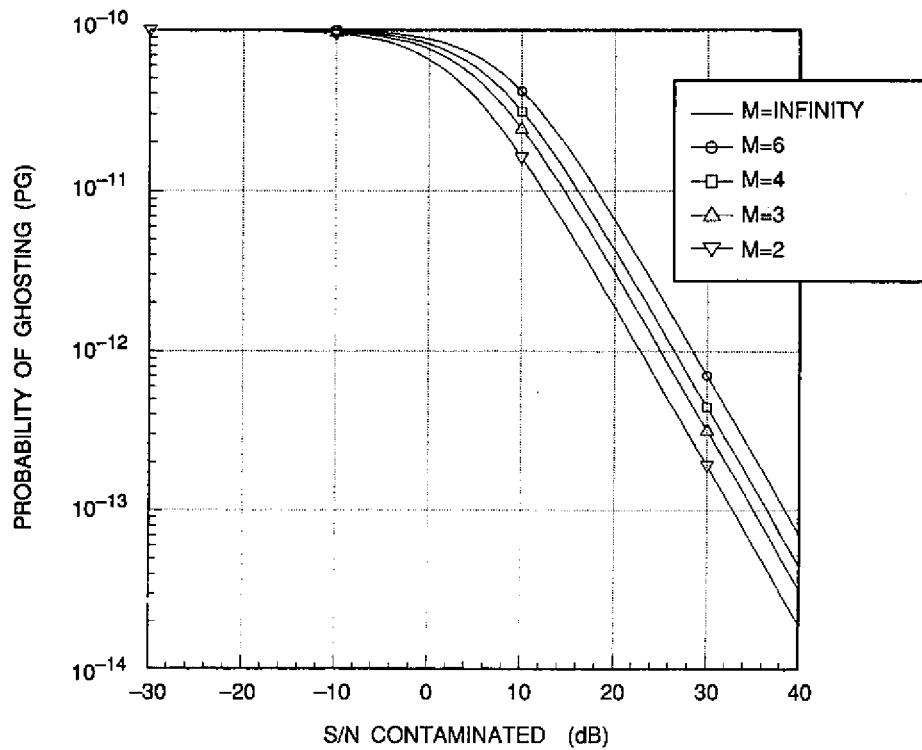


Fig. 9 — Kelly detector: PG for contaminated signal $N = 30$, $PF = 1.D-10$

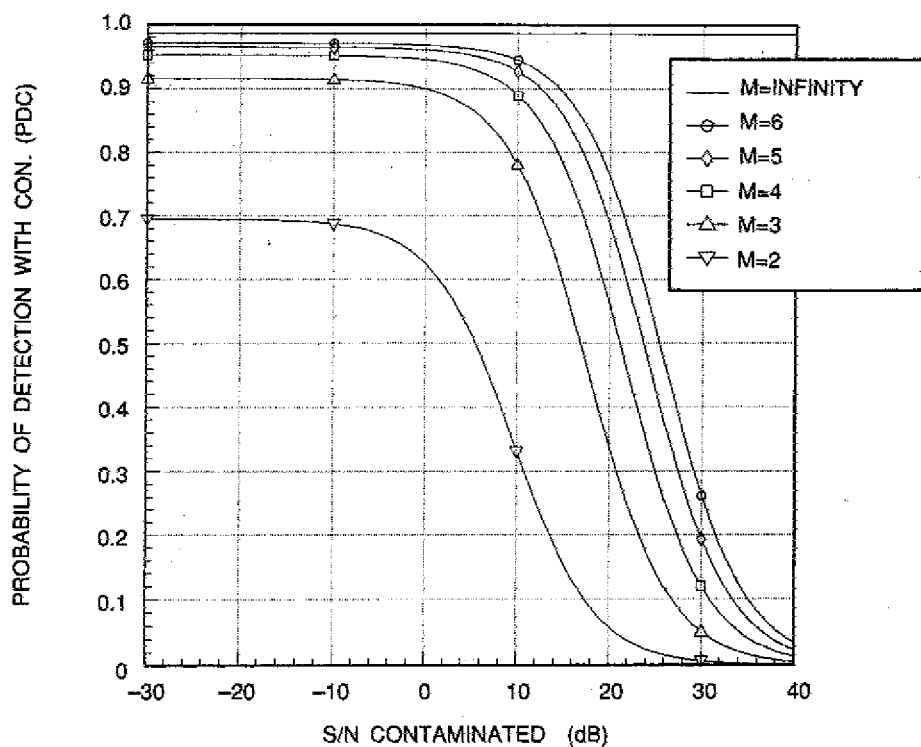


Fig. 10 — Kelly detector: PD contaminated $N = 2$, $PF = 1.D-6$, $S/N_{opt} = 30$ dB

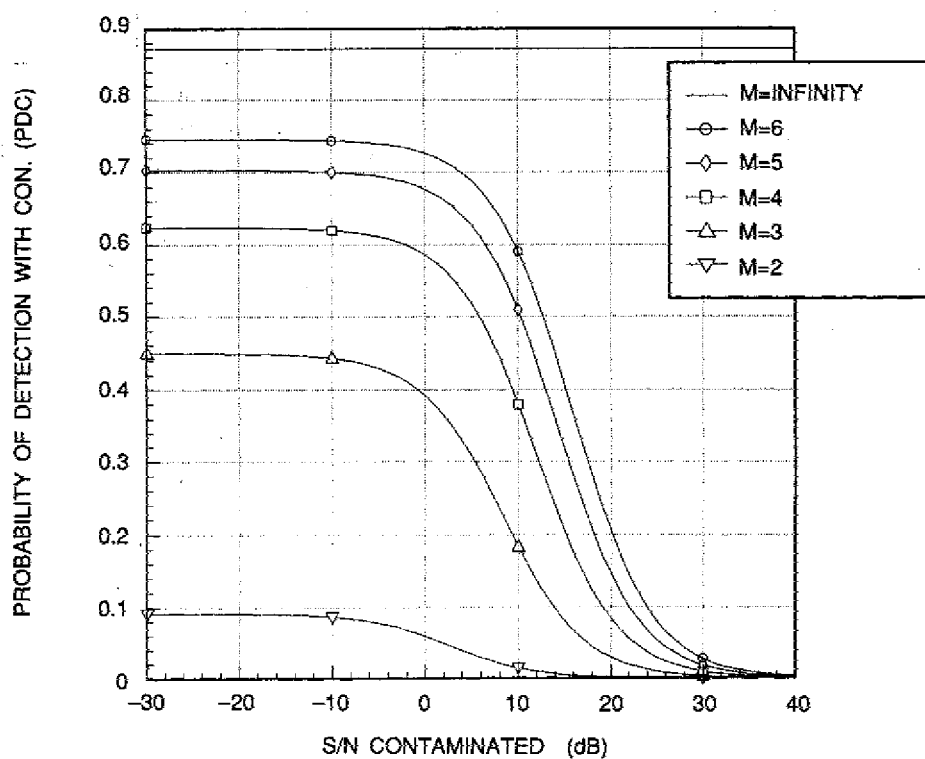


Fig. 11 — Kelly detector: PD contaminated $N = 2$, $PF = 1.D-6$, $S/N_{opt} = 20$ dB

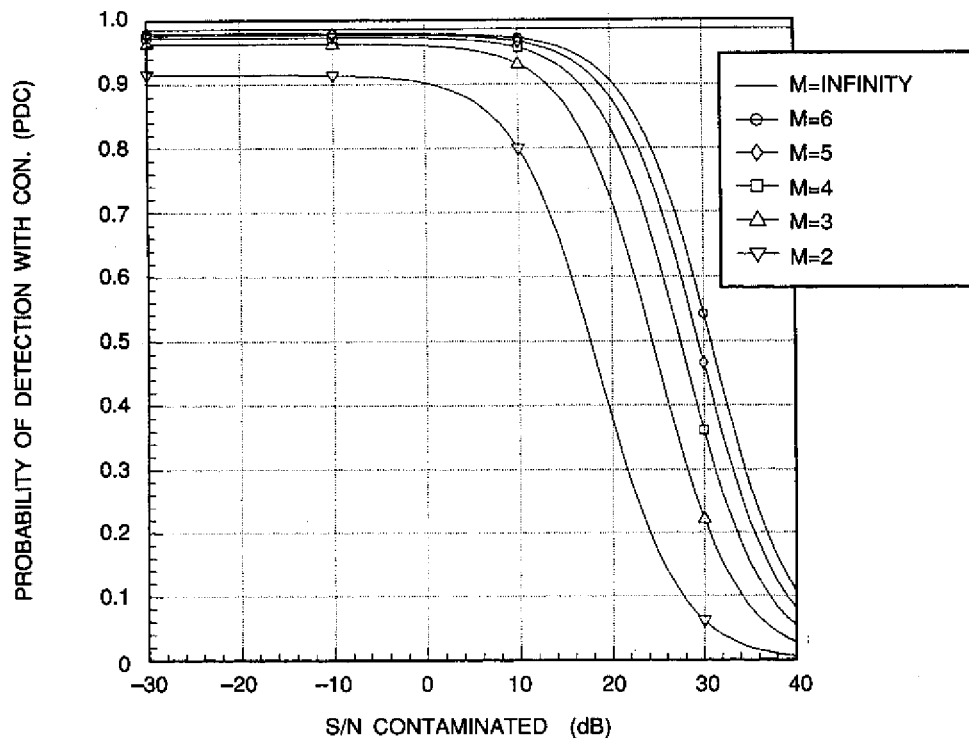


Fig. 12 — Kelly detector: PD contaminated $N = 5$, $PF = 1.D-6$, $S/N \text{ opt} = 30 \text{ dB}$

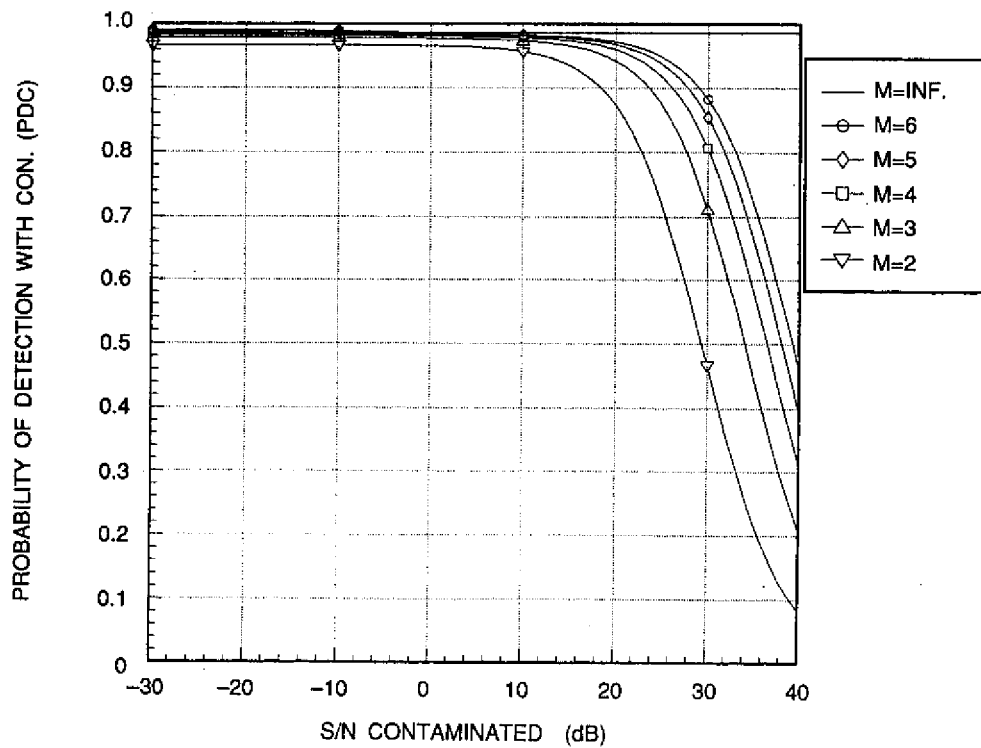


Fig. 13 — Kelly detector: PD contaminated $N = 30$, $PF = 1.D-6$, $S/N \text{ opt} = 30 \text{ dB}$

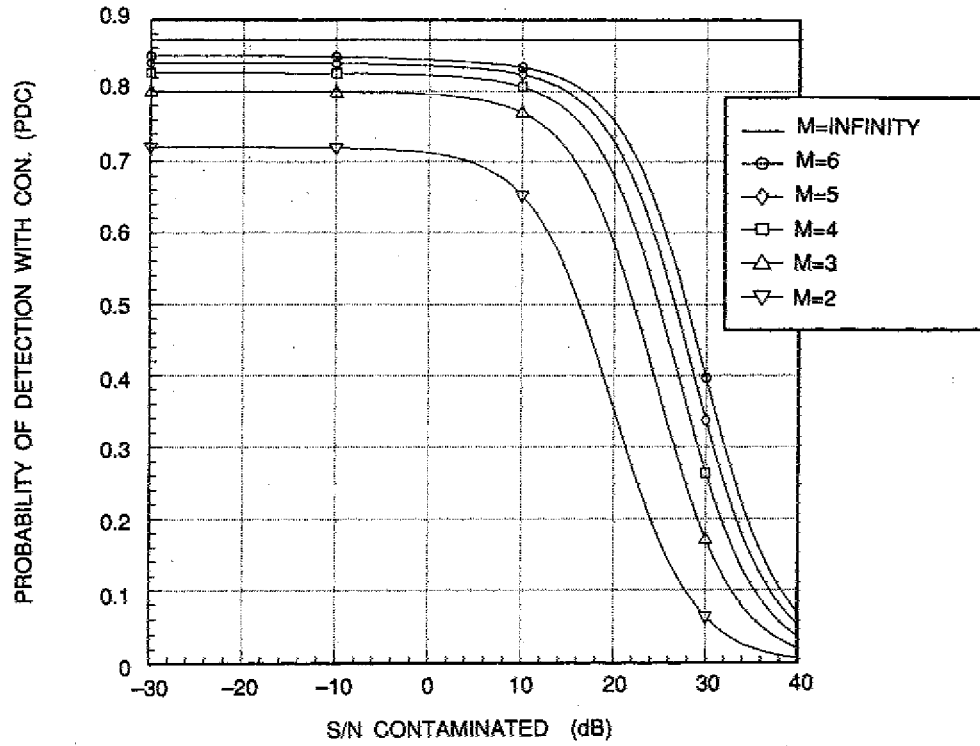


Fig. 14 — Kelly detector: PD contaminated $N = 30$, $PF = 1.D-6$, $S/N \text{ opt} = 20 \text{ dB}$

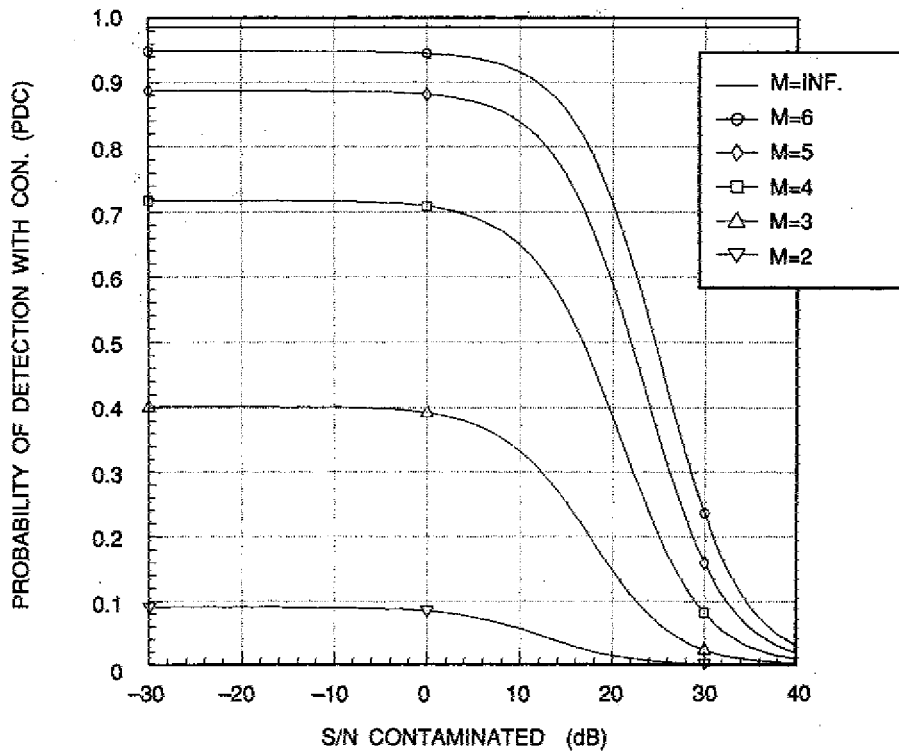


Fig. 15 — Mean level detector: PD contaminated $N = 2$, $PF = 1.D-6$, $S/N \text{ opt} = 30 \text{ dB}$

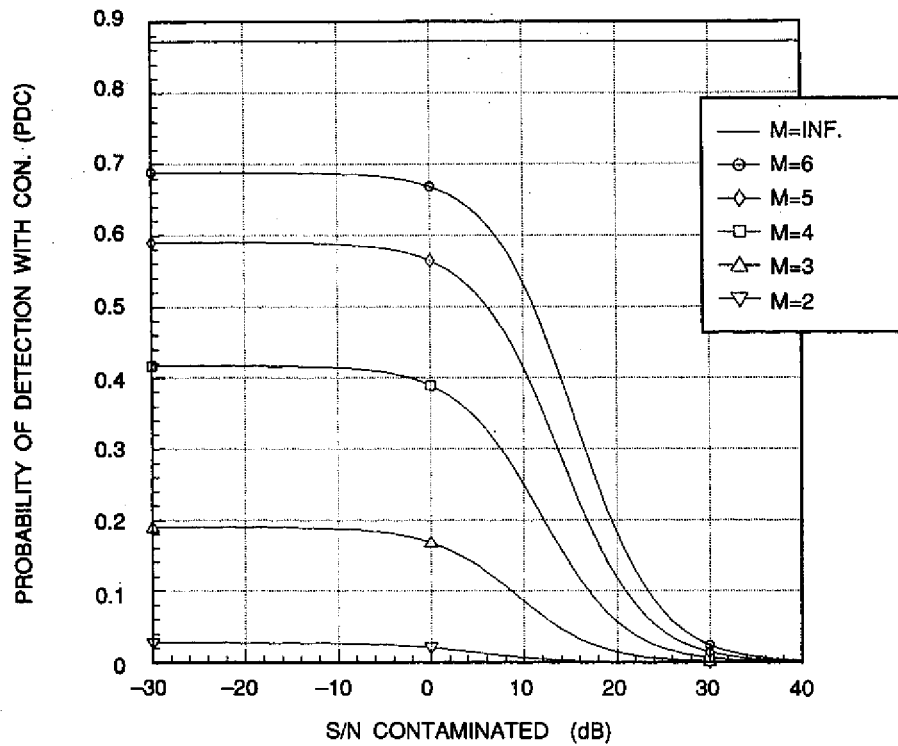


Fig. 16 — Mean level detector: PD contaminated $N = 2$, $PF = 1.D-6$, $S/N_{opt} = 20$ dB

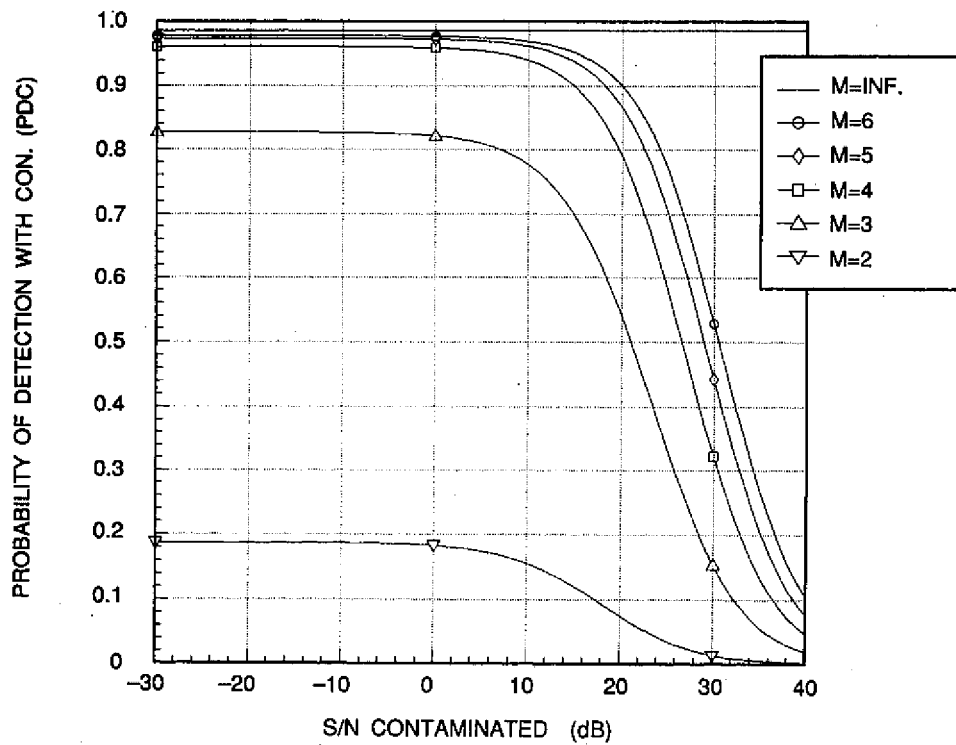


Fig. 17 — Mean level detector: PD contaminated $N = 5$, $PF = 1.D-6$, $S/N_{opt} = 30$ dB

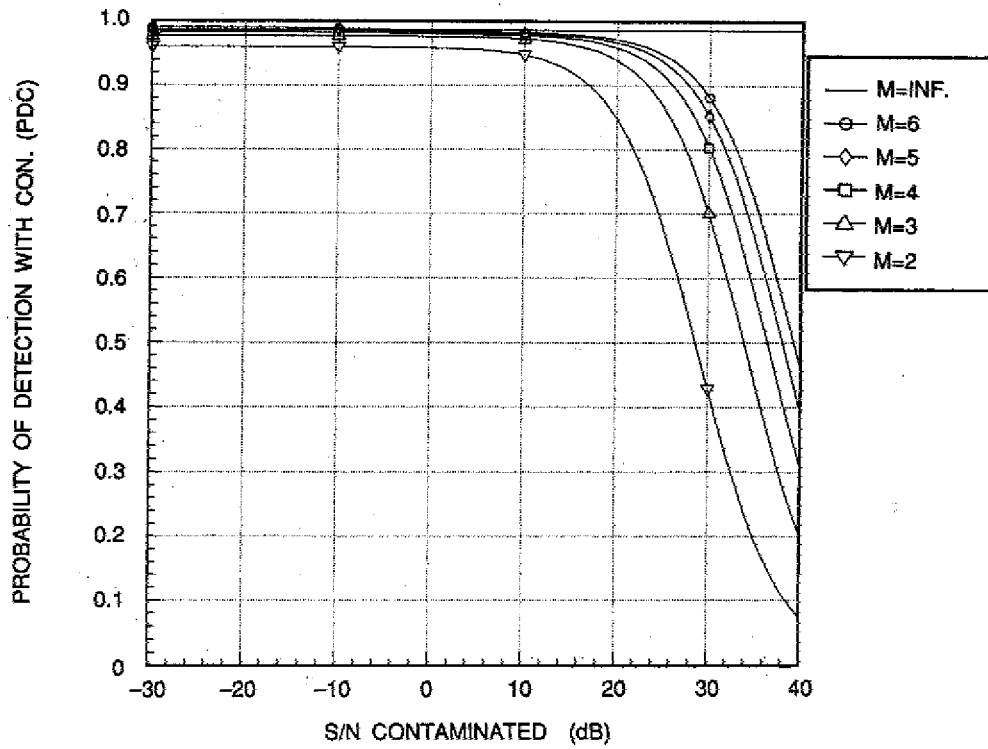


Fig. 18 — Mean level detector: PD contaminated $N = 30$, $PF = 1.D-6$, S/N opt = 30 dB

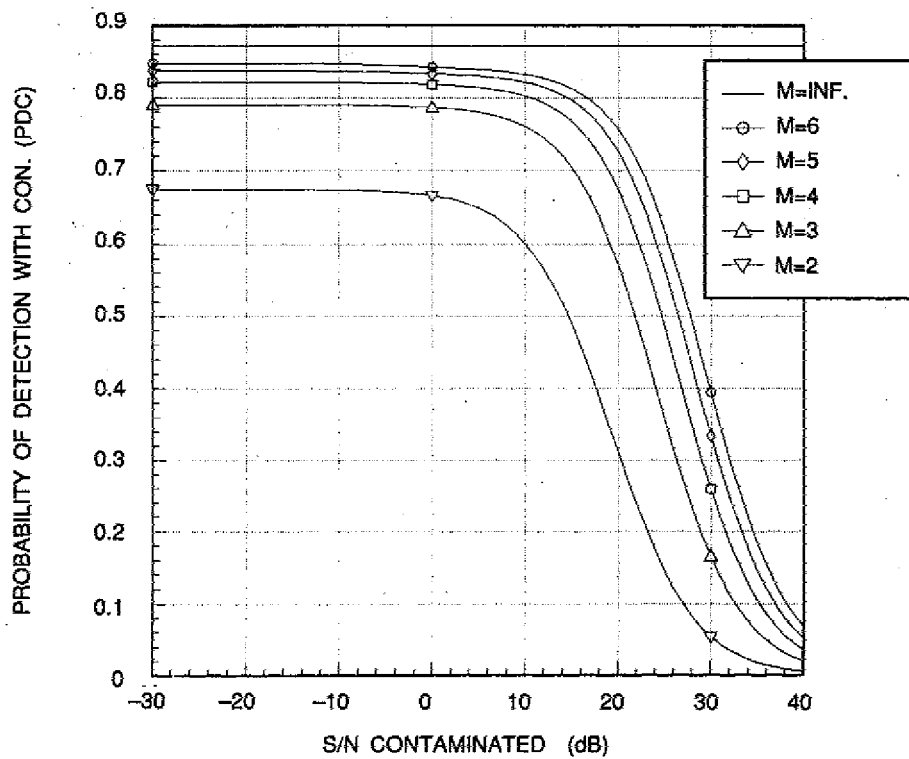


Fig. 19 — Mean level detector: PD contaminated $N = 30$, $PF = 1.D-6$, S/N opt = 20 dB

We found that the P_G performance results were identical for both the GLRT and MLAD and a given set of input parameters. Thus, we give only the P_G performance results for the GLRT. Some pertinent observations to be made from Figs. 2 through 19 are:

1. Both P_D and P_G degrade monotonically with increasing contamination $(S/N)_{con}$.
2. A small amount of contamination $((S/N)_{con} = -10 \text{ dB})$ decreases P_G . However, 10 dB of contamination is necessary make P_G decrease approximately by a factor of 10.
3. For most cases, P_D begins to significantly decrease in 10 to 20 dB of contamination.
4. For small M (2-6), the P_G 's are within a factor of five. This spread increases with increasing N .
5. As noted in Ref. 1, P_D monotonically increases with increasing M . For $(S/N)_{con} = 0$, the steady state P_D 's are indicated by the flat region of each curve.
6. For P_D , the GLRT and MLAD have similar relative performance trends.

One of the more significant results indicated by the curves is that the ghosting probability does not increase in the presence of contamination. Hence, the CFAR capability of both the GLRT and MLAD is not degraded in the sense that the false alarm probability (with contamination) is upper bounded by the quiescent false alarm probability (no contamination). However, because P_G is decreasing, inherently the detector's (MLAD or GLRT) variable threshold is increasing and, hence, the detection probability decreases.

One final note. A simple solution to decrease the effects of signal contamination is to use a large number of samples (make K or M large). However, we caution against this solution in that this was a simplified analysis where only one sample vector was contaminated. Obviously, if we take enough samples, the effects of this one sample can be significantly diminished by averaging over many samples. In reality, making K large can result in even more signal contamination, since there may be more opportunities for this to occur.

5.0 SUMMARY

Two schemes for adaptive detection, Kelly's generalized likelihood ratio test (GLRT) and the mean level adaptive detector (MLAD), have been analyzed with respect to the deleterious effect of desired signal contamination of the data used to compute the sampled covariance matrix for the two detections. This effect can occur when more than one desired signal is present in the sampled data. Detection probability P_D and false alarm performance (ghosting probability P_G) were predicted for the two schemes under the assumptions that the input noises were Gaussian random variables that were temporally independent but spatially correlated; and the desired signal's amplitude was Rayleigh distributed. P_D and P_G were computed as a function of the false alarm probability with no contamination P_F , the number of input channels, the number of independent samples-per-channel, the matched filtered output S/N power ratio, and the S/N of the contaminating desired signal. The P_D and P_F were obtained for a number of representative cases.

It was found that both P_D and P_G decreased with increasing levels of contamination. The P_G performance was almost identical for the GLRT and MLAD. The P_D performance for the two adaptive detectors showed similar relative performance trends. Significantly, it was shown that the ghosting probability does not exceed P_F in the presence of contamination. Hence, the CFAR capability of

the GLRT or MLAD is not degraded in the sense that false alarm probability is upper-bounded by the quiescent false alarm probability (no contamination).

6.0 REFERENCES

1. K. Gerlach, "Convergence Performance of Adaptive Detectors, Part 2," NRL Report 9337, Aug. 1991.
2. E.J. Kelly, "An Adaptive Detection Algorithm," *IEEE Trans. AES* **22**(1), 115-127 (1986).
3. B.O. Steenson, "Detection Performance of a Mean-Level Threshold," *IEEE Trans. AES* **4**(4), 529-534 (1968).
4. G.M. Dillard, "Mean-Level Detection of Nonfluctuating Signals," *IEEE Trans. AES* **10**(6), 795-799 (1974).
5. K. Gerlach, "Convergence Performance of Adaptive Detectors, Part 1," NRL Report 9311, July 1991.
6. I.S. Reed, J.D. Mallett, and L.E. Brennan, "Rapid Convergence Rate in Adaptive Arrays," *IEEE Trans. AES* **10**(6), 853-863 (1974).
7. J.V. Di Franco and W.L. Rubin, *Radar Detection* (Artch. House, Dedham, MA, 1980).

Appendix

THE PROBABILITY DENSITY FUNCTION (PDF) OF η

Starting with Eq. (11), we write

$$\eta = u_{22}^2 = \sum_{k=N}^{K-1} |z_{Nk}^{(N-1)}|^2 + |z_{NK}^{(N-1)}|^2, \quad (\text{A1})$$

where $z_{nk}^{(N-1)}$, $k = N+1, \dots, K-1$ are independently and identically distributed circular Gaussian random variable (r.v.) with power equal to 1, and $z_{NK}^{(N-1)}$ is a circular Gaussian r.v. with power equal to $\sigma_c^2 + 1$. Define

$$x = |z_{NK}^{(N-1)}|^2, \quad (\text{A2})$$

$$y = \sum_{k=N}^{K-1} |z_{Nk}^{(N-1)}|^2, \quad (\text{A3})$$

and

$$L = K - N. \quad (\text{A4})$$

The PDFs of x and y are given by

$$p_x(x) = \frac{1}{\sigma_c^2 + 1} \exp \left\{ -\frac{x}{\sigma_c^2 + 1} \right\}; \quad x \geq 0, \text{ and} \quad (\text{A5})$$

$$p_y(y) = \frac{1}{(L-1)!} y^{L-1} e^{-y}; \quad y \geq 0. \quad (\text{A6})$$

Now

$$\begin{aligned} p_\eta(\eta) &= \int_0^\eta p_x(\eta - \alpha) p_y(\alpha) d\alpha \\ &= \frac{1}{(L-1)!(\sigma_c^2 + 1)} \exp \left\{ -\frac{\eta}{\sigma_c^2 + 1} \right\} \int_0^\eta \alpha^{L-1} \exp \left\{ -\frac{\alpha \sigma_c^2}{\sigma_c^2 + 1} \right\} d\alpha. \end{aligned} \quad (\text{A7})$$

Set $\lambda = \alpha/\eta$. Then

$$p_\eta(\eta) = \frac{1}{(L-1)!(\sigma_c^2 + 1)} \eta^L \exp \left\{ -\frac{\eta}{\sigma_c^2 + 1} \right\} \int_0^1 \lambda^{L-1} \exp \left\{ -\frac{\lambda \eta \sigma_c^2}{\sigma_c^2 + 1} \right\} d\lambda. \quad (\text{A8})$$